THE JOURNAL OF PHYSICAL CHEMISTRY Letters

Letter

pubs.acs.org/JPCL

Coherent Oscillations in Chlorosome Elucidated by Two-Dimensional Electronic Spectroscopy

Sunhong Jun,[†,‡] Cheolhee Yang,[†,‡] Megumi Isaji,[§] Hitoshi Tamiaki,[§] Jeongho Kim,*[,∥] and Hyotcherl Ihee*[,†,‡]

[†]Center for Nanomaterials and Chemical Reactions, Institute for Basic Science (IBS), Daejeon 305-701, Republic of Korea

[‡]Department of Chemistry, KAIST, Daejeon 305-701, Republic of Korea

[§]Graduate School of Life Sciences, Ritsumeikan University, Kusatsu, Shiga 525-8577, Japan

[∥]Department of Chemistry, Inha University, Incheon 402-751, Republic of Korea

Supporting Information

ABSTRACT: Chlorosomes are the most efficient photosynthetic light-harvesting complexes found in nature and consist of many bacteriochlorophyll (BChl) molecules self-assembled into supramolecular aggregates. Here we elucidate the presence and the origin of coherent oscillations in chlorosome at cryogenic temperature using 2D electronic spectroscopy. We observe coherent oscillations of multiple frequencies superimposed on the ultrafast amplitude decay of 2D spectra. Comparison of oscillatory features in the rephasing and nonrephasing 2D spectra suggests that an oscillation of 620 cm^{-1} frequency arises from electronic coherence. However, this coherent oscillation can be enhanced by vibronic coupling with intermolecular vibrations of BChl aggregate, and thus it might originate from vibronic coherence rather than pure electronic coherence. Although the 620 cm^{-1} oscillation dephases rapidly, the electronic (or vibronic) coherence may still take part in the initial step of energy transfer in chlorosome, which is comparably fast.

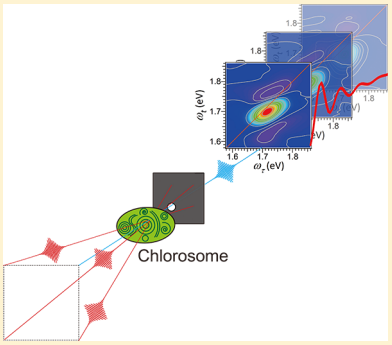

SECTION: Spectroscopy, Photochemistry, and Excited States

Chlorosomes are the largest and the most efficient light-harvesting complexes (LHCs) found in nature. They consist of hundreds of thousands of bacteriochlorophyll (BChl) molecules self-assembled into supramolecular J-type aggregates without the involvement of any protein and exhibit strong excitonic coupling among constituent BChl *c*, *d*, *e*, or *f* molecules.[1−3] The molecular architecture of chlorosomes is unique in comparison with other natural LHCs, where several pigments are held in precise positions by a protein scaffold. This unique composition of chlorosomes allows us to readily synthesize chlorosomes and their chemically modified analogues in vitro.[4] Because of the processability and highly efficient intrachlorosome energy transfer, chlorosomes are envisioned as potential building blocks of artificial photosynthesis.[5−8] There have been many efforts to characterize the structure of chlorosomes, but their large size and the presence of significant disorder prevents the structural determination at the molecular level using X-ray crystallography. From cryoelectron microscopy and NMR studies, it was proposed that BChls are organized into curved lamellar structures or multilayered rolls,[9−12] as schematically shown in Figure 1a, but the exact arrangement of BChls within chlorosomes is still in controversy.

In green sulfur bacteria, solar energy absorbed by the core of chlorosomes is transferred to the baseplate consisting of BChl *a* molecules and followed by energy transfer to the reaction center via the Fenna−Matthews−Olson (FMO) complex. The time scales of these excited-state processes in chlorosomes have been determined using time-resolved spectroscopic techniques.[13−20] Although there are some discrepancies on the assignment of the measured time constants to particular processes, it was found that a series of energy-transfer processes occur on various time scales ranging from hundreds of femtoseconds to hundreds of picoseconds, reflecting hierarchical structure of chlorosomes. For example, kinetic components on the time scale of hundreds of femtoseconds were assigned to rapid energy relaxation among the exciton states within an individual layer of BChls, while the layer-to-layer energy transfer in a chlorosome occurs on the time scale of a few picoseconds.[13−16] Then, the energy transfer from chlorosomes to the baseplate occurs in tens to hundreds of picoseconds depending on the species of chlorosome.[13,15,18] In addition to these relaxation processes, oscillations of 50−250 cm^{-1} frequencies superimposed on the time-resolved signals were observed and ascribed to coherently excited vibrational modes of the BChl aggregate.[13,17−21]

Previously, most of the time-resolved studies on chlorosomes were performed using (pump−probe) transient absorption

Received: February 14, 2014
Accepted: March 27, 2014

   dx.doi.org/10.1021/jz500328w | *J. Phys. Chem. Lett.* 2014, 5, 1386−1392

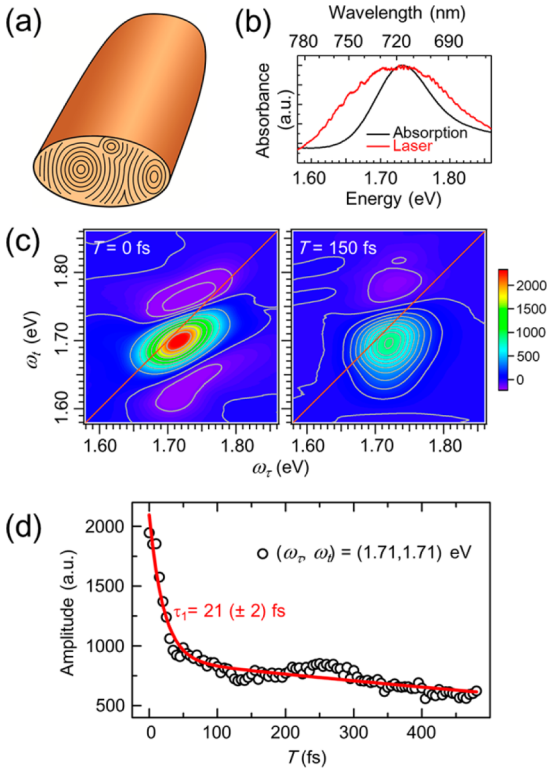

Figure 1. (a) Schematic of the structure of chlorosome. BChls are organized into either curved lamellar sheets or multilayered tubular structures.[2,10] The size of a single chlorosome is about 100 × 200 × 30 nm (width × length × height).[37,38] (b) Absorption spectrum (black line) of chlorosome from *Cba. limnaeum* measured at room temperature and the spectral profile of the laser pulse (red line) used for the 2D-ES measurement. The absorption band at 650−800 nm is ascribed to the Q_y transition of the BChl *e* chlorosome. (c) Real part of 2D spectra of chlorosome at T = 0 and 150 fs, which were measured at 77 K. We note that the Q_y transition energy slightly shifts to red at 77 K, as indicated by the position of the major peak in the 2D spectra. (d) Amplitude decay of 2D-ES signal at (ω_τ, ω_t) = (1.71, 1.71 eV) (black circles) along the T axis shown together with its double-exponential fit (red line). The faster decay component has the time constant of 21 fs. The amplitudes at other locations in the 2D spectrum also change rapidly with similar time constants. It can be clearly seen that oscillations are superimposed on the amplitude decay.

spectroscopy, whereby the transient changes of the absorption spectrum after photoexcitation are measured. In transient absorption spectra, various features arising from short-lived excited states are often overlapped to one another along a single energy axis, complicating its interpretation. In contrast, two-dimensional electronic spectroscopy (2D-ES) spreads out the excited-state absorption features into a 2D energy space (composed of absorption and emission energy axes) so that those features can be unambiguously resolved.[22,23] As a result, a 2D spectrum measured at a specific time delay after photoexcitation provides an instantaneous snapshot of electronic coupling and energy transfer among different excited states. In particular, when multiple excited states are coherently excited by a broadband pulse, complex pathways of energy flow among those states are obtained. Recently, this powerful technique has allowed us to probe the excitation energy flow in photosynthetic LHCs in real time, elucidating complex pathways and mechanism of energy transfer.[24−33] Notably, it was proposed that long-lived electronic coherence generated among electronic excited states may play a crucial role in achieving high efficiency of excitation energy transfer in natural photosynthetic LHCs,[25,26,30−33] thus negating the traditional mechanism of incoherent hopping (called Förster energy transfer). Although the identity (whether electronic or vibrational) and the exact role of the quantum coherence in photosynthetic energy transfer are still in dispute, the mechanism of energy transfer among the exciton states in LHCs has become a hot topic of investigation in association with an emerging field of quantum biology.[34,35]

Recently, 2D-ES was applied to chlorosomes (consisting of BChl *c* molecules) isolated from green sulfur bacteria, *Chlorobaculum* (*Cba.*) *tepidum* and *Chloroflexus* (*Cfl.*) *aurantiacus*, at room temperature and revealed that the ultrafast (incoherent) diffusion of excitation energy on the sub-100 fs time scale is responsible for the initial energy transfer in chlorosome.[36] In particular, any coherent oscillation was not observed in that study, leading to the conclusion that the chlorosome does not function as a coherent light-harvester. In this work, we apply the broadband 2D-ES to a different type of chlorosome (consisting of BChl *e* molecules) isolated from a green sulfur bacterium, *Cba. limnaeum* (previously called *Chlorobium phaeobacteroides*), at cryogenic temperature. In contrast with the previous 2D-ES study, we clearly observed coherent oscillations superimposed on the decay of 2D-ES signal. From Fourier analysis, we elucidated the origins of the coherent oscillations of multiple frequencies. In particular, the oscillation of ∼620 cm^{-1} frequency originates from electronic coherence, suggesting that coherent energy transfer mediated by electronic coherence may be in effect in chlorosome.

The steady-state absorption spectrum of the chlorosome consisting of BChl *e* molecules measured at room temperature is shown in Figure 1b. The absorption band at 650−800 nm is ascribed to the Q_y transition of the chlorosome. The spectrum of the laser pulse used in this experiment covers the entire Q_y absorption band. Figure 1c shows the real (absorptive) part of the 2D spectra measured at T = 0 and 150 fs. The principle and the experimental details of 2D electronic spectroscopy are described in the Supporting Information (SI). Most notably, the spectrum at T = 0 fs contains a positive peak elongated along the diagonal. This positive peak corresponds to the contributions from ground-state bleaching (GSB) and stimulated emission (SE) between the ground and the electronic excited states involved in the Q_y transition. As T increases, the shape of the positive peak rapidly changes, becoming more round in concurrence with the decreasing amplitude along the diagonal. In particular, the amplitude of the positive peak grows prominently below the diagonal, and thus the negative ESA peak below the diagonal disappears, resulting in an asymmetric peak shape with respect to the diagonal. The line shape change of the peak occurs mainly on the time scale of 20−30 fs and is completed within T = 150 fs with the peak shape staying almost the same thereafter. Considering that the layer-to-layer energy transfer takes hundreds of femtoseconds to a few picoseconds, this ultrafast change of the 2D line shape must correspond to downhill energy relaxation in a coherent domain or among coherent domains within a BChl layer, as was assigned in the previous 2D-ES study[36] and theoretical investigations[39,40] on chlorosomes. Here a coherent domain refers to a region where several BChl molecules are strongly coupled to each other and have excitonic wave functions delocalized over those coupled chromophores (that is, exciton delocalization).

dx.doi.org/10.1021/jz500328w | *J. Phys. Chem. Lett.* 2014, 5, 1386−1392

We note that the previous 2D-ES study on chlorosomes at room temperature did not report any oscillatory component in the population-time evolution of the 2D-ES signal.[36] In contrast, in our 2D spectra for chlorosomes at cryogenic temperature, we clearly see that oscillations are superimposed on the amplitude decays of the 2D-ES signal along T axis and persist over the time window of 480 fs in our measurement. (See Figure 1d.) In the initial study that proposed the involvement of quantum coherence in energy transfer in a photosynthetic LHC (FMO complex), such long-lasting oscillation of the amplitude in the 2D spectra along the population time T was regarded as the evidence of long-lived electronic coherence among the exciton states of multiple pigment chromophores.[25] However, coherent oscillation of the 2D spectra can also arise from another origin, that is, local vibrational modes, which is not directly related to the efficiency of energy transfer. Since then, there has been much dispute on the origin of the oscillation, whether it is from purely electronic or vibrational coherence and whether such quantum coherence plays any important role in efficient energy transfer of photosynthetic LHCs.[41,42] Unfortunately, the oscillations of the two different origins are supposed to appear at the same locations in the 2D spectrum, making the assignment difficult. Accordingly, several methods of distinguishing the two types of coherences,[33,43−45] or lack thereof,[46] were proposed. Thus far, the most reliable method of distinguishing the coherences of two different origins is to decompose a 2D spectrum into rephasing (R) and nonrephasing (NR) components and examine the presence of oscillations at various locations on the R and NR components.[33,43,44] The oscillation arising from electronic coherence appears only (1) at the cross peaks on the R spectrum and (2) at the diagonal peaks on the NR spectrum. In contrast, the oscillation originating from vibrational coherence appears at both cross and diagonal peaks on the R and NR spectra.

Following this comparative test between R and NR spectra, we decomposed our 2D spectra into R and NR components, as shown in Figure S2 in the SI, and examined the origin of the coherent oscillations. Because a chlorosome consists of hundreds of thousands of BChl molecules and therefore has a manifold of exciton states, it is impossible to check the presence of oscillations at specific locations on the 2D spectrum on a state-by-state basis, as was done for other smaller LHCs. Instead, to systematically check the locations where the oscillation is present distinctly, we assembled together a series of 2D spectra measured at various population times to construct a 3D data set in the (ω_τ, T, ω_t) domain and then Fourier-transformed the 3D data with respect to T to generate a 3D spectral solid in the (ω_τ, ω_T, ω_t) domain.[47] To consider only the oscillatory components that have small amplitudes relative to the overall 2D-ES signal, the Fourier transform with respect to T was performed after subtracting the exponential fit of the amplitude decay at every location in the 2D spectrum. For simplicity, instead of showing the entire 3D spectral solid, we show only the representative slices of the spectral solid, that is, 2D Fourier transform (FT) maps at selected frequencies of ω_T = 140 and 620 cm^{-1} in Figure S3a in the SI and Figure 2a, respectively. Each 2D FT map demonstrates the distribution of the oscillation of a selected ω_T frequency over the entire 2D spectrum.

Among coherent oscillations of multiple frequencies observed in our data, the most pronounced oscillation of 140 cm^{-1} frequency was found to originate from vibrational

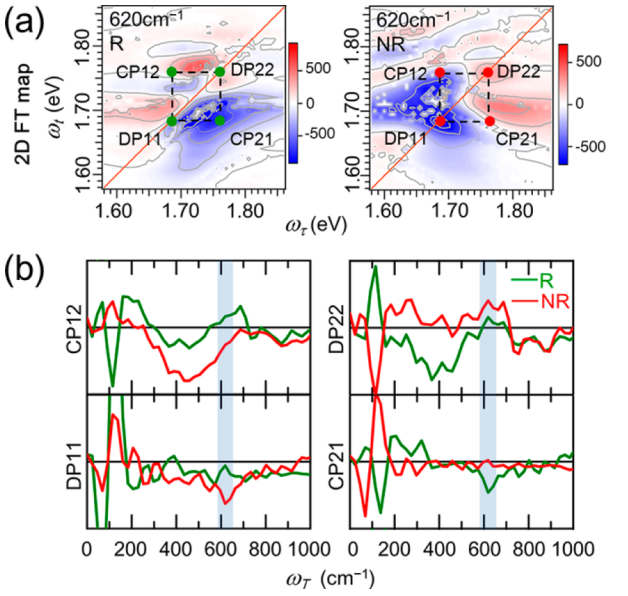

Figure 2. (a) Rephasing (left) and nonrephasing (right) 2D FT maps for the 620 cm^{-1} oscillation. (b) Line slices of the 3D spectral solid along the ω_T axis (that is, FT spectrum with respect to ω_T) for rephasing (green line) and nonrephasing (red line) components at four selected points, CP12, CP21, DP11, and DP22, on the 2D spectra as indicated by green (rephasing) and red (nonrephasing) points on the 2D FT maps shown in panel a.

coherence according to the comparative test, as described in detail in the SI. Here we focus on the oscillation of 620 cm^{-1} frequency. The R and NR components of the 2D FT maps for the 620 cm^{-1} oscillation are shown in Figure 2a. The R component has the largest amplitude at a cross-peak position below the diagonal, while the NR component shows the maximum amplitude at a diagonal-peak position with similar ω_t energy as the maximum-amplitude cross-peak position in the R component. On the basis of this observation, we examined the origin of this oscillation by looking into the line-slices of the 3D spectral solid along the ω_T axis (that is, FT spectrum with respect to ω_T) at four selected points on the 2D spectra: CP21 (1.761, 1.685 eV), DP11 (1.685, 1.685 eV), CP12 (1.685, 1.761 eV), and DP22 (1.761, 1.761 eV). The first two points, CP21 and DP11, are the locations where the R and NR components of the 2D FT map exhibit the largest amplitudes, respectively, and the latter two points are the conjugate pairs of the first two points on the 2D spectrum. We note that the difference between absorption and emission frequencies, $|\omega_\tau - \omega_t|$, is ∼620 cm^{-1} at CP21 and CP12, which is in agreement with the principle that a quantum beat of a certain frequency is expected to appear at the locations where $|\omega_\tau - \omega_t|$ matches the beat frequency.

As can be seen in Figure 2b, in the line-slices at CP21, there is clearly a (negative) peak in the ω_T frequency region of 585−655 cm^{-1} in the R component but no peak in the NR component. In contrast, in the line-slices at DP11, the NR component has a distinct (negative) peak at ∼620 cm^{-1}, but the R component does not. For the line-slices at CP12, both R and NR components have nonzero values in the frequency region of interest, but they are of opposite signs (and thus out of phase by ∼180°) to each other, indicating that they are of different origins and the R component certainly has nonzero amplitude. For DP22, the NR component has a much larger peak at 620 cm^{-1} than the R component. Summing up these

dx.doi.org/10.1021/jz500328w | J. Phys. Chem. Lett. 2014, 5, 1386−1392

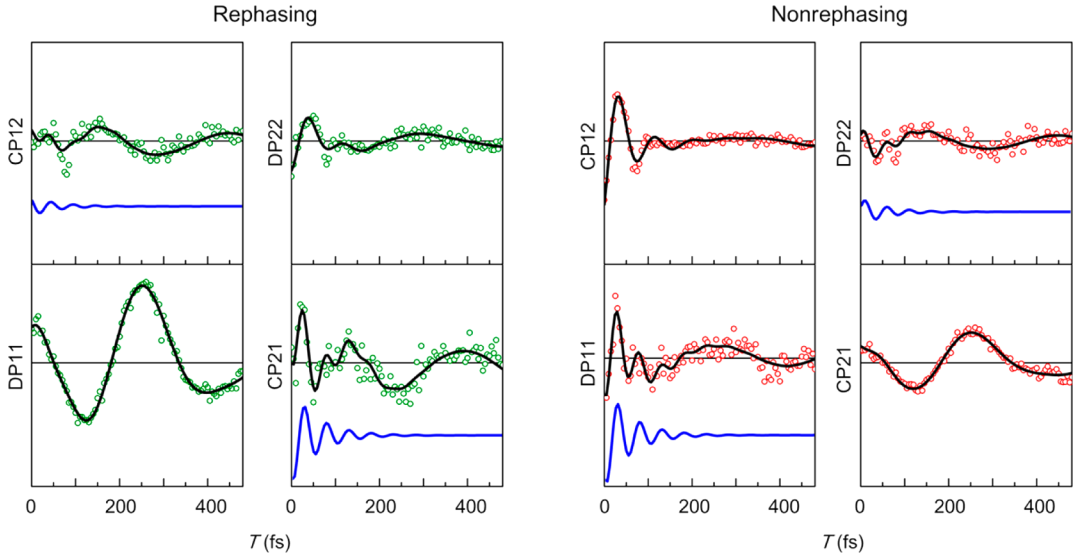

Figure 3. Time-domain traces for the rephasing (green circles) and nonrephasing (red circles) spectra and their global fits (black) at the selected points in Figure 2a. The oscillatory component of 654 cm^{-1} frequency and 60 fs dephasing time (blue) is identified only at CP21 (R), DP11 (NR), CP12 (R), and DP22 (NR).

observations, the oscillation of 620 cm^{-1} frequency is present only at the cross-peak points (CP21 and CP12) in the R component and at the diagonal-peak points (DP11 and DP22) in the NR component. Therefore, according to the comparative test, the oscillation of 620 cm^{-1} frequency presumably originates from electronic coherence.

To confirm the origin of these oscillations, we performed the linear prediction singular value decomposition (LPSVD) and the global fitting analyses for the time-domain traces at the selected points in Figure 2a. The details of the LPSVD and the global fitting analyses are described in Sections 9 and 10, respectively, in the SI, and the complete LPSVD and the global fitting parameters are listed in Table S2 and S3, respectively, in the SI. The time traces and their global fits are shown in Figure 3. From both analyses, we were able to identify an oscillatory component with the frequency of ∼620 cm^{-1} (and the dephasing time of 60 fs) only at the CPs of the R spectrum and at the DPs of the NR spectrum. We note that the oscillatory components identified for CP12 (R) and DP22 (NR) have smaller amplitudes than the ones found for CP21 (R) and DP11 (NR). This difference of the amplitudes seems to be caused by smaller signal amplitudes at CP12 and DP22, which is the general case in the 2D spectra of LHCs. (See Section 8 of the SI for details.) As expected, the frequencies of those oscillations extracted from the time-domain traces match well with $|\omega_\tau - \omega_t|$ at CP21 and CP12 within ∼85%. Thus, the comparative test between R and NR spectra suggests that the oscillation of 620 cm^{-1} frequency originates from electronic coherence. Here we note that the 620 cm^{-1} oscillation has much smaller amplitude compared with the 140 cm^{-1} oscillation. This comparison of the oscillation amplitudes supports our assignment because, in molecular aggregates, the oscillations induced by vibrational coherence are expected to be much stronger than the ones induced by electronic coherence according to a theoretical study.[45]

According to the LPSVD and global fitting analysis, the 620 cm^{-1} oscillation assigned to electronic coherence in chlorosome exhibits much shorter lifetime (60 fs) than the electronic coherence beats observed in other LHCs.[25,30,32,33] In general, such ultrashort lifetime is characteristic of electronic coherence. Specifically, the short-lived beating in chlorosome can be accounted for by several factors, for example, higher density of exciton states and relatively larger reorganization energy in chlorosomes than in other smaller LHCs. In addition, dephasing of the electronic coherence in chlorosome must be influenced by the supramolecular structure of chlorosome. Unlike other smaller LHCs, a chlorosome has significant static heterogeneity among coherent domains in a BChl layer as well as among BChl layers constituting a single chlorosome. The electronic coherence in chlorosome will be generated only within each coherent domain, where the delocalized exciton states of different energies can be coherently excited. Because of the heterogeneity among coherent domains, even slight differences in the phase of the coherence beats from many coherent domains will lead to destructive interference by ensemble averaging.[36,48,49] Therefore, 2D-ES signal measured for an ensemble of coherent domains in a chlorosome will exhibit faster dephasing than the signal measured only for a single coherent domain. Considering this additional artificial dephasing mechanism induced by heterogeneity, there is a possibility that the electronic coherence in individual coherent domains might be longer-lived than measured by 2D-ES.[49] Related to this issue, a recent theoretical study proposed that 2D-ES can significantly underestimate the lifetime of electronic coherences due to the destructive interference with several pathways that are not important for excitonic energy transfer, for example, interference with vibrational coherences.[50]

Although the comparative test between R and NR components presented above yielded a conclusion that the oscillation of 620 cm^{-1} frequency arises from electronic coherence, we cannot completely rule out the involvement of vibrational modes that are vibronically coupled to the electronic Q_y transition. In particular, we note that the oscillations examined in this work match well the vibrational frequencies (138, 276, 626 cm^{-1}, ...) of the BChl aggregate obtained from the atomistic calculation of spectral density for model chlorosomes consisting of multilayered rolls.[39] (See Figure S7 in the SI.) The vibrational frequencies that appear in the

dx.doi.org/10.1021/jz500328w | J. Phys. Chem. Lett. 2014, 5, 1386−1392

spectral density correspond to vibrational modes whose nuclear displacement can modify the excitation energy, that is, the vibrational modes with strong vibronic coupling. In particular, the vibrations in the low-frequency region below 1000 cm^{-1} are ascribed to intermolecular interactions between the BChl molecules. The 140 cm^{-1} oscillation, the most pronounced coherent oscillation in our 2D-ES data, must arise from these intermolecular vibrations in a BChl layer, in agreement with our assignment of this oscillation to vibrational coherence. The 620 cm^{-1} oscillation, which was identified to originate from electronic coherence according to the test in the previous, can also be enhanced by borrowing the oscillator strength from the intermolecular vibrations of the same frequency via vibronic coupling, and thus it might originate from vibronic coherence rather than pure electronic coherence. In fact, the role of vibrations for enhancing the energy transfer in various biological and chemical systems has attracted much interest recently.[42,51−57] In particular, this consideration can be supported by recent theoretical developments to account for the potential role of quantum coherence in photosynthetic energy transfer, for example, vibronic-exciton model.[42,51,53−55,57] According to this model, in molecular aggregates and photosynthetic LHCs, strong vibronic coupling between excitons and quantized vibrations quasi-resonant with excitonic energy gaps may significantly enhance the lifetime of coherent oscillations as well as the efficiency of energy transfer. In this regard, it would be of much interest to theoretically explore the effect of vibronic coupling on the energy transfer in chlorosome. From this perspective, it is also possible that the vibrational modes of other frequencies assist establishing electronic coherences. For example, the spectral density calculated for BChl aggregate has much larger intensities (and thus stronger vibronic coupling) in the 1500−2000 cm^{-1} region than below 1000 cm^{-1}. (See Figure S7 in the SI.) Our measurement was not able to resolve such high-frequency oscillations due to limited signal-to-noise ratio, but it might be possible to detect the high-frequency oscillations with improved temporal stability of the laser system.

Despite the rapid dephasing of the coherent oscillation arising from electronic (or vibronic) coherence, it is plausible that the coherence may still contribute to the earliest stage of energy transfer in chlorosome. According to the line-shape dynamics of the positive 2D peak presented above, the energy transfer within a coherent domain occurs on a 20−30 fs time scale. This time scale is comparable to or even shorter than the dephasing time of the coherent oscillation at 77 K. Therefore, before the coherent oscillation completely dephases, it has a good chance of completing at least one oscillatory period (= 54 fs for 620 cm^{-1} oscillation). According to theoretical investigations, a complete sampling of all possible energy transfer pathways by a full period of quantum beating and subsequent excitation trapping at an energetic minimum by rapid dephasing is the optimum condition for unidirectional and efficient coherent energy transfer.[58−60]

From the dephasing time of 60 fs at 77 K measured in this work, we can estimate the room-temperature dephasing time of ∼15 fs, assuming that the dephasing rate is linearly proportional to the temperature in the Markovian limit.[61] With the time resolution of our experiment (15 fs), it might be challenging to measure the oscillation undergoing such rapid dephasing at room temperature, which was probably the case in the previous 2D-ES study of chlorosome at room temperature.[36] The estimated dephasing time at room temperature well-matches a theoretically predicted value at 300 K by an atomistic calculation for model chlorosomes consisting of multilayered rolls.[62] Even with ∼15 fs dephasing time (= time constant of an exponential decay), the complete decay of the beating will take ∼50 fs. This time scale is long enough to complete one cycle of beating and short enough to collapse the coherence for excitation trapping at an energetic minimum. This scenario becomes more realistic when considering that the dephasing time in individual coherent domains can be longer without the previously mentioned artificial dephasing induced by heterogeneity. Therefore, the electronic (or vibronic) coherence may take part in the initial step of energy transfer in chlorosome, which is comparably fast as the dephasing of electronic coherence. However, it still needs to be investigated whether the electronic coherence enhances the rate and the efficiency of the initial ultrafast energy transfer and whether the enhancement of energy transfer rate on the ultrashort time scale influences the energy transfer on longer time scales.

In conclusion, we elucidated the presence and the origin of coherent oscillations in chlorosome from *Cba. limnaeum* at cryogenic temperature by applying 2D-ES. The result of this work provides the first evidence of quantum coherence of electronic origin observed in chlorosome and may stimulate theoretical studies that investigate the potential roles of electronic and vibrational coherences in ultrafast energy transfer in chlorosome at the microscopic level. On the experimental side, the 2D-ES experiment on single chlorosomes, where the ensemble averaging can be alleviated, will give further insights into the origin of the coherent oscillations and potential roles of quantum coherence in photosynthetic energy transfer.

■ ASSOCIATED CONTENT

Supporting Information

Structure of BChl aggregate in chlorosome. Introduction to 2D electronic spectroscopy. Experimental methods. FT resolution of 2D FT spectra. Low-frequency oscillations in 2D spectrum. Locations of low-frequency oscillation in 2D spectrum. Locations of 620 cm^{-1} oscillation in 2D spectrum. Asymmetric shape of 2D spectra. Linear prediction singular value decomposition of the oscillations. Global fitting analysis of the oscillations. 2D rephasing and nonrephasing spectra at various population times. 2D FT maps for 140 cm^{-1} oscillation and FT line-slices. Time-domain traces and LPSVD components at the selected points for low-frequency oscillations. 2D FT maps for 70 cm^{-1} oscillation. Time-domain traces and LPSVD components at the selected points for 620 cm^{-1} oscillation. Spectral density calculated for BChl aggregate. Tables listing the parameters from the LPSVD analysis of the oscillations. Table listing the fit parameters from the global fitting analysis of the oscillations. This material is available free of charge via the Internet at http://pubs.acs.org.

■ AUTHOR INFORMATION

Corresponding Authors

*J.K.: E-mail: jkim5@inha.ac.kr.
*H.I.: E-mail: hyotcherl.ihee@kaist.ac.kr.

Notes

The authors declare no competing financial interests.

■ ACKNOWLEDGMENTS

This work was supported by Institute for Basic Science (IBS) [CA1401-01]. This work was supported by an Inha University

Research Grant (INHA-48581). This work was partially supported by Grants-in-Aid for Scientific Research (A) (no. 22245030) as well as on Innovative Areas "Artificial Photosynthesis (AnApple)" (no. 24107002) from the Japan Society for the Promotion of Science (JSPS). We thank Prof. Alán Aspuru-Guzik and Dr. Takatoshi Fujita at Harvard University for helpful discussions and providing the spectral density calculated for model chlorosomes.

REFERENCES

(1) Frigaard, N.-U.; Bryant, D. A. Chlorosomes: Antenna Organelles in Green Photosynthetic Bacteria. In *Microbiology Monographs*; Shively, J., Ed.; Springer: Berlin, Germany, 2006; Vol. 2, pp 79−114.

(2) Oostergetel, G.; Amerongen, H.; Boekema, E. The Chlorosome: A Prototype for Efficient Light Harvesting in Photosynthesis. *Photosynth. Res.* **2010**, *104*, 245−255.

(3) Harada, J.; Mizoguchi, T.; Tsukatani, Y.; Noguchi, M.; Tamiaki, H. A Seventh Bacterial Chlorophyll Driving a Large Light-Harvesting Antenna. *Sci. Rep.* **2012**, *2*, 671.

(4) Shoji, S.; Hashishin, T.; Tamiaki, H. Construction of Chlorosomal Rod Self-Aggregates in the Solid State on Any Substrates from Synthetic Chlorophyll Derivatives Possessing an Oligomethylene Chain at the 17-Propionate Residue. *Chem.—Eur. J.* **2012**, *18*, 13331−13341.

(5) Roger, C.; Miloslavina, Y.; Brunner, D.; Holzwarth, A. R.; Wurthner, F. Self-Assembled Zinc Chlorin Rod Antennae Powered by Peripheral Light-Harvesting Chromophores. *J. Am. Chem. Soc.* **2008**, *130*, 5929−5939.

(6) Miyatake, T.; Tamiaki, H. Self-Aggregates of Natural Chlorophylls and Their Synthetic Analogues in Aqueous Media for Making Light-Harvesting Systems. *Coord. Chem. Rev.* **2010**, *254*, 2593−2602.

(7) Alster, J.; Polivka, T.; Arellano, J. B.; Chabera, P.; Vacha, F.; Pšenčík, J. Beta-Carotene to Bacteriochlorophyll *c* Energy Transfer in Self-Assembled Aggregates Mimicking Chlorosomes. *Chem. Phys.* **2010**, *373*, 90−97.

(8) Kataoka, Y.; Shibata, Y.; Tamiaki, H. Supramolecular Energy Transfer from Photoexcited Chlorosomal Zinc Porphyrin Self-Aggregates to a Chlorin or Bacteriochlorin Monomer as Models of Main Light-Harvesting Antenna Systems in Green Photosynthetic Bacteria. *Bioorg. Med. Chem. Lett.* **2012**, *22*, 5218−5221.

(9) Hohmann-Marriott, M.; Blankenship, R.; Roberson, R. The Ultrastructure of Chlorobium Tepidum Chlorosomes Revealed by Electron Microscopy. *Photosynth. Res.* **2005**, *86*, 145−154.

(10) Oostergetel, G. T.; Reus, M.; Gomez Maqueo Chew, A.; Bryant, D. A.; Boekema, E. J.; Holzwarth, A. R. Long-Range Organization of Bacteriochlorophyll in Chlorosomes of *Chlorobium tepidum* Investigated by Cryo-Electron Microscopy. *FEBS Lett.* **2007**, *581*, 5435−5439.

(11) Egawa, A.; Fujiwara, T.; Mizoguchi, T.; Kakitani, Y.; Koyama, Y.; Akutsu, H. Structure of the Light-Harvesting Bacteriochlorophyll *c* Assembly in Chlorosomes from *Chlorobium limicola* Determined by Solid-State NMR. *Proc. Natl. Acad. Sci. U.S.A.* **2007**, *104*, 790−795.

(12) Ganapathy, S.; Oostergetel, G. T.; Wawrzyniak, P. K.; Reus, M.; Gomez Maqueo Chew, A.; Buda, F.; Boekema, E. J.; Bryant, D. A.; Holzwarth, A. R.; de Groot, H. J. M. Alternating Syn-Anti Bacteriochlorophylls Form Concentric Helical Nanotubes in Chlorosomes. *Proc. Natl. Acad. Sci. U.S.A.* **2009**, *106*, 8525−8530.

(13) Prokhorenko, V. I.; Steensgaard, D. B.; Holzwarth, A. R. Exciton Dynamics in the Chlorosomal Antennae of the Green Bacteria *Chloroflexus aurantiacus* and *Chlorobium tepidum*. *Biophys. J.* **2000**, *79*, 2105−2120.

(14) Pšenčík, J.; Polívka, T.; Němec, P.; Dian, J.; Kudrna, J.; Malý, P.; Hála, J. Fast Energy Transfer and Exciton Dynamics in Chlorosomes of the Green Sulfur Bacterium *Chlorobium tepidum*. *J. Phys. Chem. A* **1998**, *102*, 4392−4398.

(15) Pšenčík, J.; Ma, Y.-Z.; Arellano, J. B.; Hála, J.; Gillbro, T. Excitation Energy Transfer Dynamics and Excited-State Structure in Chlorosomes of *Chlorobium phaeobacteroides*. *Biophys. J.* **2003**, *84*, 1161−1179.

(16) Martiskainen, J.; Linnanto, J.; Aumanen, V.; Myllyperkiö, P.; Korppi-Tommola, J. Excitation Energy Transfer in Isolated Chlorosomes from *Chlorobium tepidum* and *Prosthecochloris aestuarii*. *Photochem. Photobiol.* **2012**, *88*, 675−683.

(17) Savikhin, S.; Zhu, Y.; Lin, S.; Blankenship, R. E.; Struve, W. S. Femtosecond Spectroscopy of Chlorosome Antennas from the Green Photosynthetic Bacterium *Chloroflexus aurantiacus*. *J. Phys. Chem.* **1994**, *98*, 10322−10334.

(18) Savikhin, S.; van Noort, P. I.; Zhu, Y.; Lin, S.; Blankenship, R. E.; Struve, W. S. Ultrafast Energy Transfer in Light-Harvesting Chlorosomes from the Green Sulfur Bacterium *Chlorobium tepidum*. *Chem. Phys.* **1995**, *194*, 245−258.

(19) Cherepy, N. J.; Du, M.; Holzwarth, A. R.; Mathies, R. A. Near-Infrared Resonance Raman Spectra of Chlorosomes: Probing Nuclear Coupling in Electronic Energy Transfer. *J. Phys. Chem.* **1996**, *100*, 4662−4671.

(20) Ma, Y. Z.; Aschenbrucker, J.; Miller, M.; Gillbro, T. Ground-State Vibrational Coherence in Chlorosomes of the Green Sulfur Photosynthetic Bacterium *Chlorobium phaeobacteroides*. *Chem. Phys. Lett.* **1999**, *300*, 465−472.

(21) Savikhin, S.; van Noort, P. I.; Blankenship, R. E.; Struve, W. S. Femtosecond Probe of Structural Analogies between Chlorosomes and Bacteriochlorophyll *c* Aggregates. *Biophys. J.* **1995**, *69*, 1100−1104.

(22) Jonas, D. M. Two-Dimensional Femtosecond Spectroscopy. *Annu. Rev. Phys. Chem.* **2003**, *54*, 425−463.

(23) Cho, M. *Two-Dimensional Optical Spectroscopy*; CRC Press: Boca Raton, FL, 2009; p 378.

(24) Brixner, T.; Stenger, J.; Vaswani, H. M.; Cho, M.; Blankenship, R. E.; Fleming, G. R. Two-Dimensional Spectroscopy of Electronic Couplings in Photosynthesis. *Nature* **2005**, *434*, 625−628.

(25) Engel, G. S.; Calhoun, T. R.; Read, E. L.; Ahn, T. K.; Mancal, T.; Cheng, Y. C.; Blankenship, R. E.; Fleming, G. R. Evidence for Wavelike Energy Transfer through Quantum Coherence in Photosynthetic Systems. *Nature* **2007**, *446*, 782−786.

(26) Collini, E.; Wong, C. Y.; Wilk, K. E.; Curmi, P. M. G.; Brumer, P.; Scholes, G. D. Coherently Wired Light-Harvesting in Photosynthetic Marine Algae at Ambient Temperature. *Nature* **2010**, *463*, 644−647.

(27) Schlau-Cohen, G. S.; Calhoun, T. R.; Ginsberg, N. S.; Read, E. L.; Ballottari, M.; Bassi, R.; van Grondelle, R.; Fleming, G. R. Pathways of Energy Flow in LHCII from Two-Dimensional Electronic Spectroscopy. *J. Phys. Chem. B* **2009**, *113*, 15352−15363.

(28) Womick, J. M.; Moran, A. M. Exciton Coherence and Energy Transport in the Light-Harvesting Dimers of Allophycocyanin. *J. Phys. Chem. B* **2009**, *113*, 15747−15759.

(29) Myers, J. A.; Lewis, K. L. M.; Fuller, F. D.; Tekavec, P. F.; Yocum, C. F.; Ogilvie, J. P. Two-Dimensional Electronic Spectroscopy of the D1-D2-Cyt B559 Photosystem II Reaction Center Complex. *J. Phys. Chem. Lett.* **2010**, *1*, 2774−2780.

(30) Panitchayangkoon, G.; Hayes, D.; Fransted, K. A.; Caram, J. R.; Harel, E.; Wen, J.; Blankenship, R. E.; Engel, G. S. Long-Lived Quantum Coherence in Photosynthetic Complexes at Physiological Temperature. *Proc. Natl. Acad. Sci. U.S.A.* **2010**, *107*, 12766−12770.

(31) Panitchayangkoon, G.; Voronine, D. V.; Abramavicius, D.; Caram, J. R.; Lewis, N. H. C.; Mukamel, S.; Engel, G. S. Direct Evidence of Quantum Transport in Photosynthetic Light-Harvesting Complexes. *Proc. Natl. Acad. Sci. U.S.A.* **2011**, *108*, 20908−20912.

(32) Harel, E.; Engel, G. S. Quantum Coherence Spectroscopy Reveals Complex Dynamics in Bacterial Light-Harvesting Complex 2 (LH2). *Proc. Natl. Acad. Sci. U.S.A.* **2012**, *109*, 706−711.

(33) Turner, D. B.; Dinshaw, R.; Lee, K.-K.; Belsley, M. S.; Wilk, K. E.; Curmi, P. M. G.; Scholes, G. D. Quantitative Investigations of Quantum Coherence for a Light-Harvesting Protein at Conditions Simulating Photosynthesis. *Phys. Chem. Chem. Phys.* **2012**, *14*, 4857−4874.

(34) Fleming, G. R.; Scholes, G. D.; Cheng, Y. C. Quantum Effects in Biology. *Proc. Chem.* **2011**, *3*, 38−57.

(35) Lambert, N.; Chen, Y.-N.; Cheng, Y.-C.; Li, C.-M.; Chen, G.-Y.; Nori, F. Quantum Biology. *Nat. Phys.* **2013**, *9*, 10−18.
(36) Dostal, J.; Mancal, T.; Augulis, R.; Vacha, F.; Pšenčík, J.; Zigmantas, D. Two-Dimensional Electronic Spectroscopy Reveals Ultrafast Energy Diffusion in Chlorosomes. *J. Am. Chem. Soc.* **2012**, *134*, 11611−11617.
(37) Tamiaki, H.; Tateishi, S.; Nakabayashi, S.; Shibata, Y.; Itoh, S. Linearly Polarized Light Absorption Spectra of Chlorosomes, Light-Harvesting Antennas of Photosynthetic Green Sulfur Bacteria. *Chem. Phys. Lett.* **2010**, *484*, 333−337.
(38) Martinez-Planells, A.; Arellano, J.; Borrego, C.; López-Iglesias, C.; Gich, F.; Garcia-Gil, J. Determination of the Topography and Biometry of Chlorosomes by Atomic Force Microscopy. *Photosynth. Res.* **2002**, *71*, 83−90.
(39) Fujita, T.; Brookes, J. C.; Saikin, S. K.; Aspuru-Guzik, A. Memory-Assisted Exciton Diffusion in the Chlorosome Light-Harvesting Antenna of Green Sulfur Bacteria. *J. Phys. Chem. Lett.* **2012**, *3*, 2357−2361.
(40) Linnanto, J. M.; Korppi-Tommola, J. E. I. Exciton Description of Chlorosome to Baseplate Excitation Energy Transfer in Filamentous Anoxygenic Phototrophs and Green Sulfur Bacteria. *J. Phys. Chem. B* **2013**, *117*, 11144−11161.
(41) Christensson, N.; Milota, F.; Hauer, J.; Sperling, J.; Bixner, O.; Nemeth, A.; Kauffmann, H. F. High Frequency Vibrational Modulations in Two-Dimensional Electronic Spectra and Their Resemblance to Electronic Coherence Signatures. *J. Phys. Chem. B* **2011**, *115*, 5383−5391.
(42) Christensson, N.; Kauffmann, H. F.; Pullerits, T.; Mančal, T. Origin of Long-Lived Coherences in Light-Harvesting Complexes. *J. Phys. Chem. B* **2012**, *116*, 7449−7454.
(43) Cheng, Y.-C.; Fleming, G. R. Coherence Quantum Beats in Two-Dimensional Electronic Spectroscopy. *J. Phys. Chem. A* **2008**, *112*, 4254−4260.
(44) Turner, D. B.; Wilk, K. E.; Curmi, P. M. G.; Scholes, G. D. Comparison of Electronic and Vibrational Coherence Measured by Two-Dimensional Electronic Spectroscopy. *J. Phys. Chem. Lett.* **2011**, *2*, 1904−1911.
(45) Butkus, V.; Zigmantas, D.; Valkunas, L.; Abramavicius, D. Vibrational vs. Electronic Coherences in 2d Spectrum of Molecular Systems. *Chem. Phys. Lett.* **2012**, *545*, 40−43.
(46) Mančal, T.; Christensson, N.; Lukeš, V.; Milota, F.; Bixner, O.; Kauffmann, H. F.; Hauer, J. System-Dependent Signatures of Electronic and Vibrational Coherences in Electronic Two-Dimensional Spectra. *J. Phys. Chem. Lett.* **2012**, *3*, 1497−1502.
(47) Turner, D. B.; Stone, K. W.; Gundogdu, K.; Nelson, K. A. Three-Dimensional Electronic Spectroscopy of Excitons in GaAs Quantum Wells. *J. Chem. Phys.* **2009**, *131*, 144510-1−144510-8.
(48) Anna, J. M.; Ostroumov, E. E.; Maghlaoui, K.; Barber, J.; Scholes, G. D. Two-Dimensional Electronic Spectroscopy Reveals Ultrafast Downhill Energy Transfer in Photosystem I Trimers of the Cyanobacterium Thermosynechococcus Elongatus. *J. Phys. Chem. Lett.* **2012**, *3*, 3677−3684.
(49) Ishizaki, A.; Fleming, G. R. On the Interpretation of Quantum Coherent Beats Observed in Two-Dimensional Electronic Spectra of Photosynthetic Light Harvesting Complexes. *J. Phys. Chem. B* **2011**, *115*, 6227−6233.
(50) Kreisbeck, C.; Kramer, T.; Aspuru-Guzik, A. Disentangling Electronic and Vibronic Coherences in Two-Dimensional Echo Spectra. *J. Phys. Chem. B* **2013**, *117*, 9380−9385.
(51) Womick, J. M.; Moran, A. M. Vibronic Enhancement of Exciton Sizes and Energy Transport in Photosynthetic Complexes. *J. Phys. Chem. B* **2011**, *115*, 1347−1356.
(52) Jordan, M. W.; Brantley, A. W.; Norbert, F. S.; Andrew, M. M. Vibronic Effects in the Spectroscopy and Dynamics of C-Phycocyanin. *J. Phys. B: At., Mol. Opt. Phys.* **2012**, *45*, 154016.
(53) Kolli, A.; O'Reilly, E. J.; Scholes, G. D.; Olaya-Castro, A. The Fundamental Role of Quantized Vibrations in Coherent Light Harvesting by Cryptophyte Algae. *J. Chem. Phys.* **2012**, *137*, 174109.
(54) Chin, A. W.; Prior, J.; Rosenbach, R.; Caycedo-Soler, F.; Huelga, S. F.; Plenio, M. B. The Role of Non-Equilibrium Vibrational Structures in Electronic Coherence and Recoherence in Pigment-Protein Complexes. *Nat. Phys.* **2013**, *9*, 113−118.
(55) Chenu, A.; Christensson, N.; Kauffmann, H. F.; Mančal, T. Enhancement of Vibronic and Ground-State Vibrational Coherences in 2D Spectra of Photosynthetic Complexes. *Sci. Rep.* **2013**, *3*, 2029.
(56) Richards, G. H.; Wilk, K. E.; Curmi, P. M. G.; Quiney, H. M.; Davis, J. A. Coherent Vibronic Coupling in Light-Harvesting Complexes from Photosynthetic Marine Algae. *J. Phys. Chem. Lett.* **2012**, *3*, 272−277.
(57) Tiwari, V.; Peters, W. K.; Jonas, D. M. Electronic Resonance with Anticorrelated Pigment Vibrations Drives Photosynthetic Energy Transfer Outside the Adiabatic Framework. *Proc. Natl. Acad. Sci. U.S.A.* **2013**, *110*, 1203−1208.
(58) Rebentrost, P.; Mohseni, M.; Kassal, I.; Lloyd, S.; Aspuru-Guzik, A. Environment-Assisted Quantum Transport. *New J. Phys.* **2009**, *11*, 033003.
(59) Caruso, F.; Chin, A. W.; Datta, A.; Huelga, S. F.; Plenio, M. B. Highly Efficient Energy Excitation Transfer in Light-Harvesting Complexes: The Fundamental Role of Noise-Assisted Transport. *J. Chem. Phys.* **2009**, *131*, 105106.
(60) Rebentrost, P.; Mohseni, M.; Aspuru-Guzik, A. Role of Quantum Coherence and Environmental Fluctuations in Chromophoric Energy Transport. *J. Phys. Chem. B* **2009**, *113*, 9942−9947.
(61) Rebentrost, P.; Chakraborty, R.; Aspuru-Guzik, A. Non-Markovian Quantum Jumps in Excitonic Energy Transfer. *J. Chem. Phys.* **2009**, *131*, 184102.
(62) Fujita, T.; Huh, J.; Saikin, S.; Brookes, J.; Aspuru-Guzik, A. Theoretical Characterization of Excitation Energy Transfer in Chlorosome Light-Harvesting Antennae from Green Sulfur Bacteria. *Photosynth. Res.* **2014**, DOI: 10.1007/s11120-014-9978-7.